2004

Friction Factor Under Transient Flow Condition

Fernando A. Ribas
Embraco

Cesar J. Deschamps
Federal University of Santa Catarina

FRICTION FACTOR UNDER TRANSIENT FLOW CONDITION

F. A. RIBAS JR[1], C. J. DESCHAMPS[2]

[1]EMBRACO
Joinville, SC, Brazil
E-mail: Fernando_A_Ribas@embraco.com.br

[2]Federal University of Santa Catarina, Dept. Mechanical Engineering
Florianopolis, SC, Brazil
E-mail: deschamps@nrva.ufsc.br

ABSTRACT

The modeling of transient flow in suction and discharge systems plays an important role in the simulation of reciprocating compressors. Frequently, a one-dimensional formulation is adopted for the governing equations, with the wall shear stress being evaluated from friction factor correlations developed for stationary flow conditions. The present work reports a numerical analysis of fully developed pulsating flow through pipes, designed to investigate transient effects on the flow velocity profile and wall shear stress. A finite volume methodology is employed to integrate and solve the differential equations, with turbulence being taken into account through the 'eddy' viscosity k-ε v^2f model of Durbin (1991). Flow field results are presented for different transient conditions and discussed in the paper. The presence of transients is seen to affect the wall shear stress to such an extent that friction factor correlations developed for stationary condition are no longer valid.

1. INTRODUCTION

The physical understanding of transient flows is a requirement in the development and optimization of several applications, such as compressors, I.C. engines, turbomachineries, etc. The fully developed periodic pipe flow in which the flow rate is forced to vary sinusoidally with time around a mean value represents one of the simplest flows under this category and, therefore, it is a natural choice for basic studies of unsteady flows.

One of the first works reported on pulsating flow is that of Uchida (1956), in which an analytical solution was obtained for a fully developed laminar pulsating flow through a pipe. Despite its relevance towards the understanding of the phenomenon, it should be noted that the turbulent flow regime prevails in virtually all technological applications. Since turbulence is not open to an analytical treatment, numerical modeling and experimental investigation are the only alternatives.

A number of experimental investigations have been done in the past 20 years considering pulsating fully developed turbulent flow in pipes (Ramaprian and Tu, 1983; Tu and Ramaprian, 1983; Mao and Hanratty, 1986; Finnicum and Hanratty, 1988; Barker and Williams, 2000). An important result from such works shows that the wall shear stress can vary out of phase in relation to the flow rate. The phase difference changes monotonically from zero degree in the quasi steady flow condition to approximately 45 degrees at high pulsating frequencies. Another interesting finding shows a departure of the velocity profile from the log law in the wall region. This is a critical aspect for turbulence modeling approaches that use wall functions to avoid solving the viscous sublayer region. Finally, a relaminarization process has been observed when the flow undergoes a strong acceleration. This phenomenon is associated with the confinement of the shear layer within the viscous sublayer, causing turbulence production to vanish. As a consequence, the flow can not maintain its turbulent regime and laminarizes even at high Reynolds number. The prediction of this flow feature is crucial because it will affect heat transfer and shear stress at the wall.

Ohmi *et al*. (1978), Kita *et al*. (1980), Tu and Ramaprian (1983) and Mao and Hanratty (1986) showed that algebraic turbulence models cannot satisfactorily predict pulsating flows. This failure has been attributed mainly to the absence of transport equations for turbulence quantities, as well as transient terms, in their formulation. To

circumvent this problem, Ismael and Cotton (1996) used a transport turbulence model, represented by the k-ε model of Launder and Sharma (1974), obtaining a fair agreement with experimental data at low frequency situations.

The present work further investigates the turbulence modeling of pulsating turbulent flows, using the k-ε v^2f model of Durbin (1991). Results for velocity profile and Reynolds shear stress are compared to experimental data to assess the model capability to predict the flow. Additionally, the friction factor is analyzed for different transient flow conditions.

2. TURBULENCE MODELING

The flow is considered to be fully developed, turbulent, incompressible and undergoing a pulsating condition represented by a harmonically oscillation of the flow rate as follows:

$$U_{m(t)} = \overline{U}_m(1+\gamma\cos\omega t) \tag{1}$$

where $U_{m(t)}$ is the mean axial velocity varying with time t, $\overline{U}_m$ is the mean phase average axial velocity, γ is the amplitude of oscillation and ω (= $2\pi f$) is the circular frequency. It should be kept in mind that in the present work the over bar symbol stands for time-mean quantity.

The URANS (Unsteady Reynolds Average Navier Stokes equation) for the axial component of the momentum equation reads

$$\frac{\partial U}{\partial t} = -\frac{1}{\rho}\frac{dp}{dx} + \frac{1}{r}\frac{\partial}{\partial r}\left[r\left(\nu\frac{\partial U}{\partial r} - \overline{uv}\right)\right] \tag{2}$$

where U, dp/dx, and $\overline{uv}$ are axial velocity, pressure gradient and Reynolds shear stress, respectively. The values of U and $\overline{uv}$ are functions of radial position and time, whereas the pressure gradient is a function of time only. The density ρ and the kinematic viscosity ν (= μ/ρ) are considered to be constants.

The Reynolds stress $\overline{uv}$, required to close Equation (2), is modeled based on the eddy viscosity hypothesis, that is

$$-\overline{uv} = \nu_t\frac{\partial U}{\partial r} \tag{3}$$

where ν_t is the turbulence viscosity. Equations (2) and (3) are solved subject to the constraint that the mean velocity $U_{m(t)}$ at any instant t should satisfy the continuity equation expressed by Equation (1).

The evaluation of the turbulence viscosity, ν_t, is carried out through the k-ε v^2f model of Durbin (1991), which is an alternative to eddy-viscosity models and the RSM. The v^2f model is similar to the standard k-ε model, but incorporates near-wall turbulence anisotropy and non-local pressure-strain effects. It is a general low Reynolds number turbulence model that is valid all the way up to solid walls, and therefore does not need to make use of wall functions. Although the model was originally developed for attached or mildly separated boundary layers, it also accurately simulates flows dominated by separation.

The v^2f model is a four equation model that solves, in addition to k and ε, a differential equation for the Reynolds stress $\overline{v^2}$ normal to the streamline and an elliptic relaxation function f. According to Durbin (1991), the v^2f model is capable to predict the near wall region more accurately than standard k-ε models because close to the wall turbulence is anisotropic, with $\overline{v^2}$ being the most affected stress by the wall proximity. Therefore, solving for $\overline{v^2}$ represents an adequate way of describing the near wall region.

The v^2f equations may be written as

$$\frac{\partial k}{\partial t} = P_k + \frac{1}{r}\frac{\partial}{\partial r}\left[r(\nu + \nu_t)\frac{\partial k}{\partial r}\right] - \varepsilon \tag{4}$$

$$\frac{\partial \varepsilon}{\partial t} = \frac{C'_{\varepsilon 1}\, P_k - C_{\varepsilon 2}\, \varepsilon}{T} + \frac{1}{r}\frac{\partial}{\partial r}\left[r\left(\nu + \frac{\nu_t}{\sigma_\varepsilon}\right)\frac{\partial \varepsilon}{\partial r}\right] \tag{5}$$

$$\frac{\partial \overline{v^2}}{\partial t} = kf - \frac{\overline{v^2}}{k}\varepsilon + \frac{1}{r}\frac{\partial}{\partial r}\left[r(\nu + \nu_t)\frac{\partial \overline{v^2}}{\partial r}\right] \tag{6}$$

$$f - L^2\left(\frac{\partial^2 f}{\partial r^2} + \frac{1}{r}\frac{\partial f}{\partial r}\right) = (C_1 - 1)\left(\frac{2/3 - \overline{v^2}/k}{T}\right) + C_2\frac{P_k}{k} \tag{7}$$

The turbulence kinetic production term, P_k, for the one-dimensional situation considered here read as

$$P_k = \nu_t\left(\frac{\partial U}{\partial r}\right)^2 \tag{8}$$

The distinguishing feature of the v^2f model is the use of the velocity scale, $\overline{v^2}$, instead of the turbulent kinetic energy, k, to evaluate the eddy viscosity:

$$\nu_t = C_\mu \overline{v^2} T \tag{9}$$

This element of the model has shown to provide the right scaling in representing the damping of turbulent transport close to the wall, which cannot be offered by the kinetic energy k.

The turbulence length and time scales, L and T, appearing in the above equations are estimated through the following relations:

$$L = C_L \max\left[L';\ C_\eta\left(\nu^3/\varepsilon\right)^{1/4}\right] \quad ; \text{with} \quad L' = \min\left(\frac{k^{3/2}}{\varepsilon}\ ;\ \frac{1}{\sqrt{3}}\ \frac{k^{3/2}}{\overline{v^2}\, C_\mu \sqrt{P_k/\nu_t}}\right) \tag{10}$$

$$T = \min\left(T'\ ;\ \frac{\alpha}{\sqrt{3}}\ \frac{k}{\overline{v^2}\, C_\mu \sqrt{P_k/\nu_t}}\right) \quad ; \text{with} \quad T' = \max\left(\frac{k}{\varepsilon};\ 6\,(\nu/\varepsilon)^{1/2}\right) \tag{11}$$

The model constants are $C_\mu = 0.22$, $C_L = 0.25$, $C_\eta = 85.0$, $\alpha = 0.6$, $C_1 = 1.4$, $C_2 = 0.3$, $C_{\varepsilon 2} = 1.9$, $\sigma_\varepsilon = 1.3$. Yet the coefficient $C'_{\varepsilon 1}$ is determined from:

$$C'_{\varepsilon 1} = 1.4\left[1 + 0.045\left(k/\overline{v^2}\right)^{1/2}\right] \tag{12}$$

3. NUMERICAL METHODOLOGY

A finite volume methodology has been employed to integrate the governing differential equations, with a fully implicit time discretization scheme applied to unsteady terms. The elliptic equation for f is not a transport equation and for this reason has been discretized via a finite difference approach. The system of algebraic equations that result from the integration over each control volume is solved with the Tridiagonal Matrix Algorithm (TDMA).

A staggered grid arrangement has been adopted, with scalar properties (k, ε, ν_t) positioned at the centre of the control volume and velocity located at the volume faces, avoiding any interpolation of convective terms at the volume faces. Since the v^2f model solve the flow up to the wall, an adequate grid refinement across the viscous sublayer is required. Launder (1984) suggests the grid should have between 20 and 30 volumes in the viscous affected region; i.e. $0 < y^+ < 50$; where y^+ (= u*y/ν) is a dimensionless distance to the wall and u* (= $\sqrt{\tau_w/\rho}$) is the friction velocity. A schematic view of the computational grid is given in Figure (1), with the solution domain limited by the wall surface and the axis of symmetry.

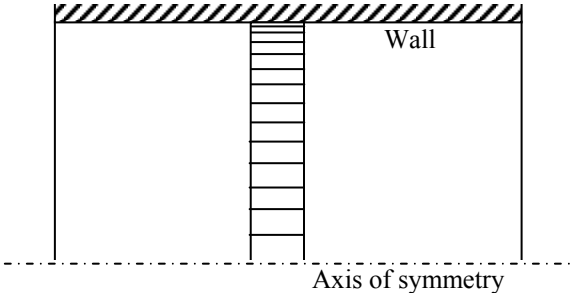

Figure 1: Computational grid and solution domain.

The solution procedure starts by solving Equation (2) and follows with a correction of the pressure gradient to satisfy the mass flow given by Equation (1). Then, the eddy viscosity ν_t is evaluated from the v^2f model and the procedure is repeated until convergence is reached in each time step. Under relaxation is required to avoid divergence of the iterative procedure. Further details on the methodology can be found in Ferziger and Peric (1996).

Boundary conditions for the governing equations are required at the wall and axis of symmetry. At the wall, the condition of no-slip and impermeable wall boundary condition are imposed; this implies that U, k and $\overline{v^2}$ are set to zero. On the other hand, the values for ε and f are set to the volume adjacent to the wall according to $\varepsilon = 2\nu k/y^2$ and $f = -20\,\nu^2\,\overline{v^2}\,/\,(\varepsilon y^4)$, respectively, where y is the distance to the wall. In the symmetry locations the normal gradients of all quantities are set to zero, with the exception of f, which is evaluated from:

$$f\big|_{r\to 0} = (C_1 - 1)\left(\frac{2/3 - \overline{v^2}/k}{T}\right) + C_2\,\frac{P_k}{k} \tag{13}$$

The v^2f equations, constant values and boundary conditions specified in this work are based on Manceau *et al*. (2000) and Behnia *et al*. (1999).

A very important aspect addressed in this work is the validation of the numerical solution by means of sensitivity tests with respect to grid refinement and time step. The computational grid used in all simulations had 138 nodes distributed according to an aspect ratio of 1.03, with the first node adjacent to the wall located at $y^+ \cong 0.5$.

4. RESULTS

Ramaprian and Tu (1983) and Tu and Ramaprian (1983) investigated a pulsating water flow through a pipe with a diameter of 50 mm at Reynolds number Re (=$\overline{U}_m$ D/ν) of 50 000, for two conditions of amplitude γ and frequency f:

i) $\gamma = 0.64$; f = 0.5 Hz and ii) $\gamma = 0.15$; f = 3.6 Hz. The authors classified the unsteady flow into 5 regimes, based on the value of $\omega D/u^*$, which is the turbulent Stokes number, and the Reynolds number. The 'quasi-steady regime' happens for $\omega D/u^* < 0.1$ and can be solved as a succession of steady flows. In the 'low-frequency regime' ($0.1 < \omega D/u^* < 1$) the flow departs from quasi-steady behavior, with the effect of the flow oscillation being spread across the entire shear layer. The turbulent structure is not affected and a quasi-steady turbulence model can still be used to predict the flow. However, it is necessary to perform a time-dependent calculation to predict the time history of the flow. The 'intermediate-frequency regime' ($1 < \omega D/u^* < 10$) is characterized by some interaction between the turbulence structure and the imposed unsteadiness. Quasi-steady turbulence models will begin to fail and become increasingly unsatisfactory as $\omega D/u^*$ increases. The structural equilibrium of turbulence may begin to break down at least in part of the cycle. The flow situation at 0.5 Hz considered by Ramaprian and Tu (1983) corresponds to $\omega D/u^* \cong 3$. At the 'high-frequency regime' ($10 < \omega D/u^* < 100$) the imposed oscillation will interact strongly with turbulent bursting process at the wall. The time-mean velocity will be affected and can exhibit an inflective profile near the wall. The periodic flow will also be affected but this effect is confined to a thin region next to the wall, beyond which the flow oscillates like a solid mass. The turbulence structure will show total departure form equilibrium. Quasi-steady turbulence models breaks down completely. Yet, calculations based on such models still predict the periodic flow in the outer layer reasonably well, since the turbulent shear-stress term in this region is almost negligible compared with the pressure-gradient term. In other words, the periodic flow in the outer region behaves like an inviscid flow. The pulsating flow at 3.6 Hz gives $\omega D/u^* \cong 20$ and, therefore, falls into this category. Finally, at $\omega D/u^*$ typically of the order of 100, a regime called the 'rapid-oscillation regime' will prevail. The interaction between the imposed oscillation and the turbulence structure will be very strong. The effect on the periodic flow will be confined to a very thin layer (~ 0.01 D) near the wall.

Figure (2) shows the present numerical results for Reynolds shear stress ($\overline{uv}/U_m^2$) compared to the experimental data of Tu and Ramaprian (1983) in different angle positions of the cycle; represented by 0^o, 45^o, 90^o, 135^o (deceleration) and 180^o, 225^o, 270^o and 315^o (acceleration). The large variation observed for the Reynolds shear stress near the wall is associated to the flow acceleration and deceleration near the wall. By examining the figure, one can clearly see a reduction in the levels of Reynolds stress in the acceleration period, probably associated to the relaminarization process explained earlier.

Predictions returned by the v^2f model agree well with the experimental data for the intermediate frequency situation (f=0.5Hz), as can be seen from Figure (2a). Numerical results obtained with the Low Reynolds Number k-ε model (Launder and Sharma, 1974) and the k-ω model (Wilcox, 1994) do not display the same level of agreement (Ribas Jr. and Deschamps, 2003). The v^2f model performs better than other eddy viscosity models in this frequency situation (f = 0.5 Hz) because transients are taken into account in the evaluation of turbulence scales. For instance, time and length scales in the near wall region are smaller than in the core region of the flow and, therefore, they are less sensitive to flow transients than those with of greater time scales. The presence of a transport equation for the normal Reynolds stress $\overline{v^2}$ in the v^2f allows the inclusion of transient effects directly on the eddy viscosity evaluation. The damping functions adopted by k-ε and k-ω models for the near wall region were not developed for unsteady problems, and their use are therefore questionable in transient situations.

Figure (2b) reveals however that for the high frequency case (f=3.6 Hz) the v^2f model fails to capture the shear stress variation, predicting a "frozen" structure, even though with a level that is in line with the time mean value indicated by the experimental data. This inconsistency has also been observed with the k-ε and k-w models, implying that the eddy viscosity hypothesis is not adequate for such transients.

Figure (3) shows velocity profiles at the wall region for γ=0.64 and f=0.5 Hz, at different angle positions along the cycle, using wall-layer variables u^+ (=U/ u*) and y (= u*y/ν), where $u^* = \sqrt{\tau_w/\rho}$. A can be observed, the velocity profiles do not follow the universal logarithmic law profile. There is a global distortion of the velocity profiles due to the varying phase shift between the local flow and the wall shear stress. Hence, the wall shear stress as a scaling parameter loses physical significance in this flow condition. This feature, captured by the v^2f model, exposes the limitation of high Reynolds number turbulence models that adopt wall functions to bridge the turbulent region to the wall. Although not shown here, for the high frequency (f=3.6 Hz) the departure from the log law is not so marked because the effect of the oscillation is confined to a thin layer next to the wall.

Figure (4) shows predictions of friction factor f ($=\tau_w/\rho V^2$) for different pulsating conditions, represented by the Strouhal number S_{tr} ($=\omega D/\overline{U}_m$), at two levels of Reynolds number. The results represent the ratio between friction factor obtained here (f_{trans}), and the stationary friction factor (f_{stat}) evaluated according to Blasius correlation:

$$f = \frac{0.3164}{Re^{1/4}} \tag{14}$$

For extremely low frequencies, the friction factor f_{trans} should agree well with that of stationary flow, represented by Equation (14), and the relation $f_{trans}/f_{trans} = 1$ (100%). As the frequency is increased, the discrepancy between the two factors becomes apparent, with the predicted f_{trans}/f_{trans} forming a closed curve, whose area is proportional to the frequency. The strong effect of flow transients on the friction factor can be attributed to inertia and relaminarization effects. In the period of deceleration, values of f_{trans} are smaller than those for stationary flow, and vice versa during the acceleration. For high frequencies ($S_{tr} = 14.02$), Figure (4) shows that even a negative friction factor may occur as a consequence of a reversal flow close to the wall. In terms of time-mean average, the friction factor decreases as the flow oscillation becomes higher. It can also be observed that the increase of the mass flow rate, represented by the Reynolds number, inhibits transient effects on the friction factor.

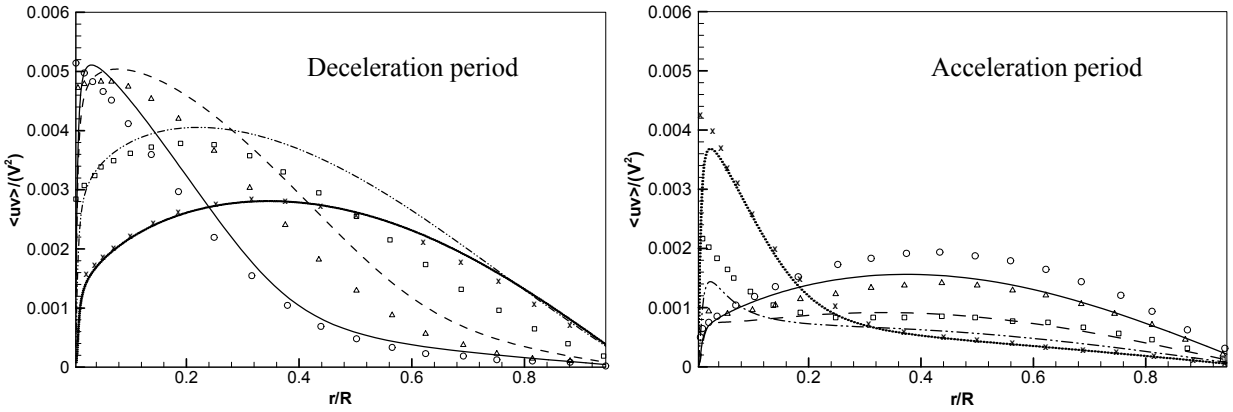

(a) γ=0.64 and f=0.5 Hz (ωD/u* ≅ 3).

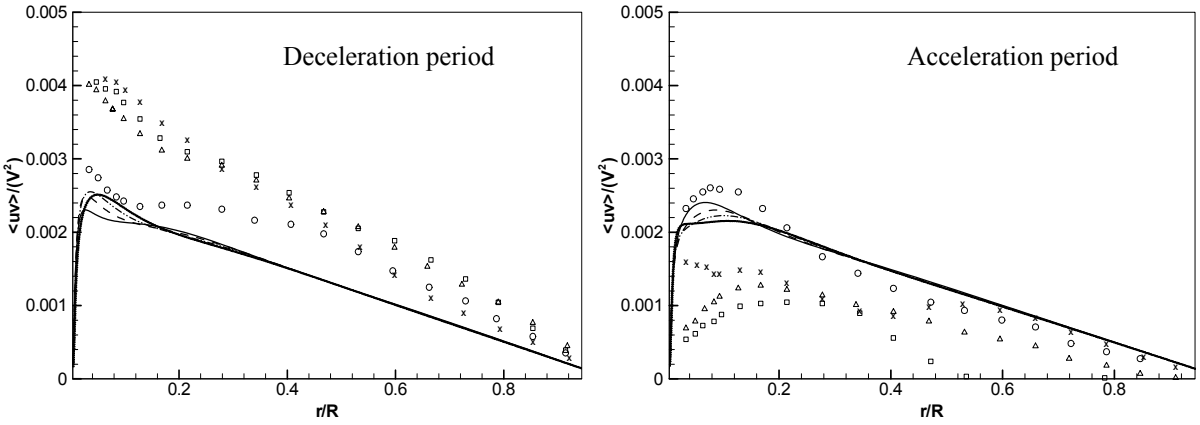

(b) γ=0.15 and f=3.6 Hz (ωD/u* ≅ 20).

Figure 2: Numerical results for Reynolds-shear stress compared to experimental data (Tu and Ramaprian, 1983);
Deceleration period: o, —— θ=0° Δ, ——— θ=45° □, —·— θ=90° ×, ····· θ=135°
Acceleration period: o, —— θ=180° Δ, ——— θ=225° □, —·— θ=270° ×, ····· θ=315°

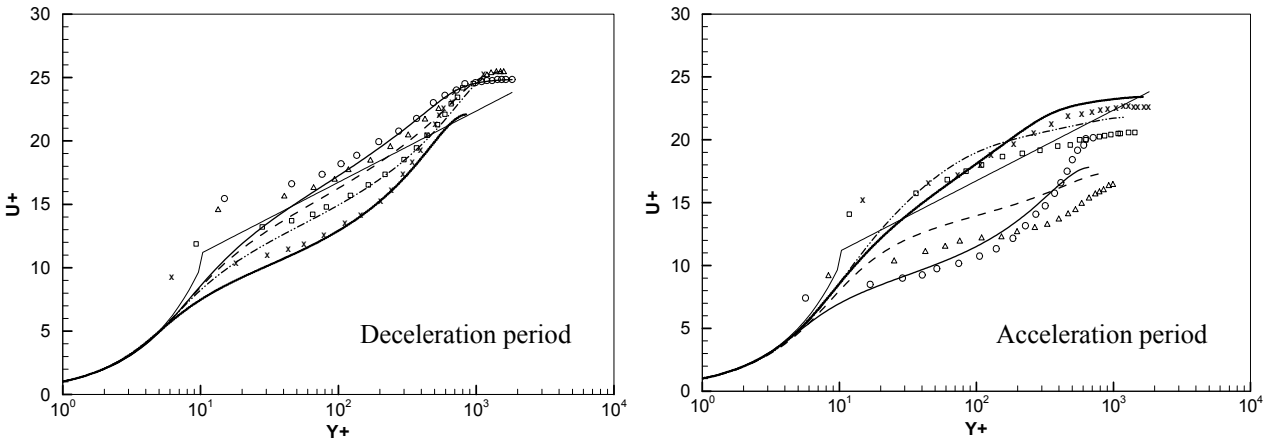

Figure 3: Numerical results and experimental data (Tu and Ramaprian, 1983) for velocity profiles in the wall region: γ=0.64 and f=0.5 Hz ($\omega D/u^* \cong 3$).

Deceleration period: o, —— θ=0° Δ, – – – θ=45° □, —·— θ=90° ×, ····· θ=135°

Acceleration period: o, —— θ=180° Δ, – – – θ=225° □, —·— θ=270° ×, ····· θ=315°

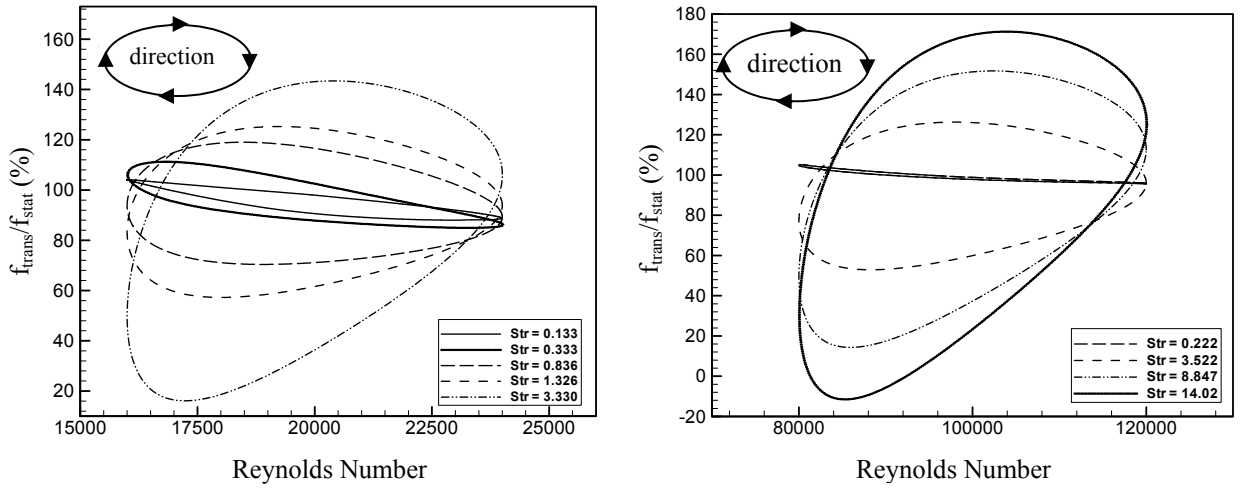

Figure 4: Friction factor for pulsating flow.

5. CONCLUSIONS

A numerical analysis of the physical behavior of pulsating turbulent flow has been presented, with turbulence contribution being estimated through the k-ε v^2f model. The v^2f model is valid all the way up to solid walls, not requiring the use of wall functions. This is an important feature since the logarithmic velocity profile does not hold for transient flows. Results obtained with the v^2f model are seen to be in good agreement with experimental data at intermediate frequency, which can be attributed to the model capability of taking into account transient terms in the evaluation of time and length scales. However, as the frequency is increased the model fails to reproduce the turbulence structure. This flaw can be foreseen to happen in all models based on the eddy viscosity concept. Wall shear stress is strongly affected by flow transients, varying out of phase in relation to the flow rate; therefore friction factor correlations devised for stationary flow are not adequate. Investigation of pulsating flow under a wider range of Reynolds and Strouhal numbers can give further insight of the phenomenon and provide data for a new friction factor correlation suitable for transient flows. The analysis can also be extended to include heat transfer since transients will also have an impact on the Nusselt number (Barker and Williams, 2000).

REFERENCES

Barker, A. R, Williams, J. E. F., 2000, Transient measurements of the heat transfer coefficient in unsteady turbulent pipe flow, *Int. J. Heat and Mass Transfer*, vol. 43, p. 3197-3207.

Behnia, M., Parneix, S., Shabany, Y., Durbin, P. A., 1999, Numerical study of turbulent heat transfer in confined and unconfined impinging jets, *Int. J. Heat and Fluid Flow*, vol. 20, p. 1-9.

Durbin, P.A., 1991, Near-wall turbulence closure modeling without "damping functions. *Theoret. Comput. Fluid. Dynamics*, no. 3, p. 1-13.

Ferziger, J.H. and Peric, M., *Computational Methods for Fluid Dynamics*, Springer-Verlag, 1996.

Finnicum, D. S., Hanratty, T. J., 1988, Influence of imposed flow oscillations on turbulence, *PCH*, vol. 10, p. 585-598.

Ismael, J. O., Cotton, M. A, 1996, Calculations of wall shear stress in harmonically oscillated turbulent pipe flow using a low-Reynolds-number k-ε model, *J. Fluid Eng*., vol. 118, pp. 189-194.

Kita, Y., Adachi, Y., Hirose, K., 1980, Periodically oscillating turbulent flow in a pipe, *Bulletin of the JSME*, vol. 23, no. 179, p. 656-664.

Launder, B. E., Sharma, B. I., 1974, Application of the energy dissipation model of turbulence to the calculation of flow near a spinning disc, *Letters in Heat and Mass Transfer*, vol. 1, p. 131-138.

Launder, B. E., 1984, Numerical computation of convective heat transfer in complex turbulent flows: time to abandon wall functions? *Int. J. Heat and Mass Transfer*, vol.9, pp. 1485-1491.

Mao, Z. X., Hanratty, T., 1986, Studies of the wall shear stress in a turbulent pulsating pipe flow, *J. Fluid. Mech*., vol. 170, p. 545-564.

Manceau, R., Parneix, S., Laurence, D., 2000, Turbulent heat transfer predictions using v^2f model on unstructured meshes, *Int. J. Heat and Fluid Flow*, vol. 21, p. 320-328.

Ohmi, M., Kyomen, S., Usui, T., 1978, Analysis of velocity distribution in pulsating turbulent pipe flow with time-dependent friction velocity, *Bulletin of the JSME*., vol. 21, no. 157, p. 1137-1143.

Ramaprian, B. R., Tu, S. W., 1983, Fully developed periodic turbulent pipe flow. Part 2. The detailed structure of the flow, *J. Fluid Mech*., vol. 137, p. 59-81.

Ribas Jr, F. A., Deschamps, C. J., 2003, Computational Simulation of Pulsating Turbulent Flow in Pipes, *Proc. 17th Int. Cong. Mech. Engineering*, São Paulo, Brazil, Paper 0409 (CD-ROM), 7 p.

Tu, S. W., Ramaprian, B. R., 1983, Fully developed periodic turbulent pipe flow. Part 1. Main experimental results and comparison with predictions, *J. Fluid Mech*., vol. 137, p. 31-58.

Uchida, S., 1956, The pulsating viscous flow superposed on the steady laminar motion of incompressible fluid in a circular pipe, *ZAMP*, vol. 10, p. 403-422.

Wilcox, D. C., 1994, *Turbulence Modeling for CFD*, DCW Industries.

ACKNOWLEDGEMENT

This work is part of a technical-scientific program between Federal University of Santa Catarina and EMBRACO. Support from the Brazilian Research Council, CNPq, is also appreciated.